Electronic version of an article published as International Journal of Bifurcation and Chaos Vol. 12, No. 5, 2002, 1111-1119,
DOI: 10.1142/S0218127402004942 © World Scientific Publishing Company, https://www.worldscientific.com/worldscinet/ijbc

Controlling Chaos in a State-Dependent Nonlinear System

Takuji Kousaka*
Dept. Electronic and Electrical Engineering,
Fukuyama University, Hiroshima, 729-0292, Japan
Tetsushi Ueta†
Dept. Information Science & Intelligent Systems,
The University of Tokushima, Tokushima, 770-8506, Japan
and
Hiroshi Kawakami‡
Dept. Electrical and Electronic Engineering,
The University of Tokushima, Tokushima, 770-8506, Japan

November 15, 2001

In this paper, we propose a general method for controlling chaos in a nonlinear dynamical system containing a state-dependent switch. The pole assignment for the corresponding discrete system derived from such a non-smooth system via Poincaré mapping works effectively. As an illustrative example, we consider controlling the chaos in the Rayleigh-type oscillator with a state-dependent switch, which is changed by the hysteresis comparator. The unstable 1- and 2-periodic orbits in the chaotic attractor are stabilized in both numerical and experimental simulations.

1 Introduction

In recent years, the study of chaotic nonlinear dynamical systems has seen rapid expansion and particularly the subject of controlling chaos has received considerable attention toward engineering applications. Since there are an infinite number of the unstable periodic orbits (UPOs) are embedded in a chaotic attractor, the general concept of controlling chaos is how to stabilize an inherent UPO by applying a small parameter perturbation to the chaotic system. It is observed that many current approaches in accomplishing this task are based on the OGY method [Ott *et al.*, 1990], after which various effective control methods have also been developed [Hunt, 1991, Pyragas, 1992, Chen & Dong, 1993, Ueta & Kawakami, 1995].

On the other hand, there have been numerous theoretical and experimental investigations on controlling chaos for piecewise linear systems [Poddar *et al.*, 1995, Saito & Mitsubori, 1995, Bernardo & Chen, 1999, Bueno & Marrero, 2000, Bernardo, 2000, Kousaka *et al.*, 2001]. However, there are very few methods being developed in the literature for controlling chaos in systems with a non-smooth nonlinearity.

*E-mail:kousaka@fuee.fukuyama-u.ac.jp
†E-mail:tetsushi@is.tokushima-u.ac.jp
‡E-mail:kawakami@ee.tokushima-u.ac.jp

For the control of such systems, we propose a general method that can stabilizes an UPO embedded in a nonlinear dynamical system containing a state-dependent switch. The basic idea of this method is based on our previous work [Ueta & Kawakami, 1995], where we proposed a stabilization method for UPOs of nonautonomous systems. However, this piece of work only considers the continuous systems with insufficient experimental results. In this paper, we further modify and extend this method and apply it to discontinuous systems.

First, we derive a composite discrete mapping as the Poincaré mapping. By using the Newton and Runge-Kutta methods, we can calculate the Jacobian and the associate differential equation, from which we can obtain the location of unstable periodic points (UPPs) of the system. Using this information, the controller is then designed with the conventional linear control technique.

Next, we consider experimental control of a specific piecewise nonlinear system, using which we describe the control method in detail. We explain the behavior of the circuit and the design of the controller with a composite Poincaré mapping.

Finally, we show how to stabilize the unstable 1- and 2-periodic orbits of the chaotic attractor by both numerical and experimental simulations.

2 Construction of the Controller

Consider m autonomous differential equations:

$$\frac{d\boldsymbol{x}}{dt} = \boldsymbol{f}_k(\boldsymbol{x}, \boldsymbol{\lambda}, \boldsymbol{\lambda}_k), \quad k = 0, 1, 2 \cdots, m-1, \tag{1}$$

where, $t \in \boldsymbol{R}$, $\boldsymbol{x} \in \boldsymbol{R}^n$. $\boldsymbol{\lambda} \in \boldsymbol{R}^r$ is a common parameter for $\boldsymbol{f}_0, \boldsymbol{f}_1, \ldots, \boldsymbol{f}_{m-1}$ and $\boldsymbol{\lambda}_k \in \boldsymbol{R}^s$ is a parameter depending only on $\boldsymbol{f}_k$. Assume that $\boldsymbol{f}_k$ is a C^∞-class map for any variables and parameters.

Define the local section Π_k given by a scalar function q_k:

$$\Pi_k = \{\boldsymbol{x} \in \boldsymbol{R}^n \,|\, q_k(\boldsymbol{x}) = 0\} \quad k = 0, 1, 2 \ldots, m-1. \tag{2}$$

When the orbit, which started from the local section Π_k, passes the local section Π_{k+1}, the equation will change from $\boldsymbol{f}_k$ to $\boldsymbol{f}_{k+1}$. This action can be easily realized by a state-dependent switch.

Assume that each solution of Eq. (1) is:

$$\begin{aligned} &\boldsymbol{x}_k(t) = \boldsymbol{\varphi}_k(t, \boldsymbol{x}_{k-1}, \boldsymbol{\lambda}, \boldsymbol{\lambda}_k) \\ &\boldsymbol{x}_k = (x_{k1}, x_{k2}, \ldots, x_{kn})^\top. \end{aligned} \tag{3}$$

Figure 1 shows the behavior of the trajectory.

Based on the above conditions, define the following m mappings:

$$\begin{array}{lllll} T_0: & \Pi_0 & \to & \Pi_1 \\ & \boldsymbol{x}_0^* & \mapsto & \boldsymbol{x}_1^* = \boldsymbol{\varphi}_0(\tau_0(\boldsymbol{x}_0^*), \boldsymbol{x}_0^*, \boldsymbol{\lambda}^*, \boldsymbol{\lambda}_0^*), \\ T_1: & \Pi_1 & \to & \Pi_2 \\ & \boldsymbol{x}_1^* & \mapsto & \boldsymbol{x}_2^* = \boldsymbol{\varphi}_1(\tau_1(\boldsymbol{x}_1^*), \boldsymbol{x}_1^*, \boldsymbol{\lambda}^*, \boldsymbol{\lambda}_1^*), \\ & & \cdots & \\ T_{m-1}: & \Pi_{m-1} & \to & \Pi_0 \\ & \boldsymbol{x}_{m-1}^* & \mapsto & \boldsymbol{x}_0^* = \boldsymbol{\varphi}_{m-1}(\tau_{m-1}(\boldsymbol{x}_{m-1}^*), \boldsymbol{x}_{m-1}^*, \boldsymbol{\lambda}^*, \boldsymbol{\lambda}_{m-1}^*), \end{array} \tag{4}$$

where the motion of the switch depends on the state of Eq. (1).

Note that the unstable fixed point exists locally on both sides of the switching manifold. This means that the system flow is continuous inside each region, but is discontinuous on the switching manifold.

Assume that this orbit has a chaotic attractor, $\boldsymbol{x}_k^*$, which is an unstable fixed point in the chaotic attractor, and use $\boldsymbol{\lambda}_0$ as the controlling parameter. The period of the unstable 1-periodic orbit is obtained as

$$\tau = \sum_{k=0}^{m-1} \tau_k. \tag{5}$$

Now, we can treat system (1) as the discrete system (4). We then try to stabilize the specified 1-periodic UPO by adding a control input, $\boldsymbol{u}$, during one mapping among every m mappings. The variational equation around the fixed point is described by the following relationship:

$$\begin{aligned}
&\boldsymbol{x}(k) = \boldsymbol{x}_m^* + \boldsymbol{\xi}(k), \quad \boldsymbol{\lambda}(k) = \boldsymbol{\lambda}_0^* + \underline{\boldsymbol{u}(k)},\\
&\boldsymbol{x}(k+1) = \boldsymbol{x}_1^* + \boldsymbol{\xi}(k+1), \quad \boldsymbol{\lambda}(k+1) = \boldsymbol{\lambda}_1^*,\\
&\boldsymbol{x}(k+2) = \boldsymbol{x}_2^* + \boldsymbol{\xi}(k+2), \quad \boldsymbol{\lambda}(k+2) = \boldsymbol{\lambda}_2^*,\\
&\cdots\\
&\boldsymbol{x}(k+m-1) = \boldsymbol{x}_{m-1}^* + \boldsymbol{\xi}(k+m-1), \; \boldsymbol{\lambda}(k+m-1) = \boldsymbol{\lambda}_m^* - 1,\\
&\boldsymbol{x}(k+m) = \boldsymbol{x}_m^* + \boldsymbol{\xi}(k+m), \; \boldsymbol{\lambda}(k+m) = \boldsymbol{\lambda}_0^* + \underline{\boldsymbol{u}(k+m)},\\
&\cdots .
\end{aligned} \tag{6}$$

The corresponding difference equations derived from every T_k mapping are written as

$$\begin{aligned}
&\boldsymbol{\xi}(k+1) = \boldsymbol{A}_m\boldsymbol{\xi}(k) + \underline{\boldsymbol{B}_m\boldsymbol{u}(k)},\\
&\boldsymbol{\xi}(k+2) = \boldsymbol{A}_1\boldsymbol{\xi}(k+1),\\
&\qquad\cdots\\
&\boldsymbol{\xi}(k+m-1) = \boldsymbol{A}_{m-2}\boldsymbol{\xi}(k+m-2),\\
&\boldsymbol{\xi}(k+m) = \boldsymbol{A}_{m-1}\boldsymbol{\xi}(k+m-1),\\
&\boldsymbol{\xi}(k+m-1) = \boldsymbol{A}_m\boldsymbol{\xi}(k+m) + \underline{\boldsymbol{B}_m\boldsymbol{u}(k+m)},
\end{aligned} \tag{7}$$

where $\boldsymbol{A}_k$ and $\boldsymbol{B}_k$ show the derivatives with respect to the initial value and the parameter $\boldsymbol{\lambda}_k$, respectively.

$$\begin{aligned}
\boldsymbol{A}_k &= \left.\frac{\partial T_k}{\partial \boldsymbol{x}_{\boldsymbol{k}}^{\boldsymbol{*}}}\right|_{t=\tau_k, \boldsymbol{x}=\boldsymbol{x}_k^*, \boldsymbol{\lambda}=\boldsymbol{\lambda}^*, \boldsymbol{\lambda}_k=\boldsymbol{\lambda}_k^*},\\
\boldsymbol{B}_k &= \left.\frac{\partial T_k}{\partial \boldsymbol{\lambda}_{\boldsymbol{k}}}\right|_{t=\tau_k, \boldsymbol{x}=\boldsymbol{x}_k^*, \boldsymbol{\lambda}=\boldsymbol{\lambda}^*, \boldsymbol{\lambda}_k=\boldsymbol{\lambda}_k^*},\\
&\quad k = 0, 1, 2, \cdots, m-1.
\end{aligned} \tag{8}$$

By utilizing the periodicity of the switching action, we define the composite Poincaré map by

$$T = T_0 \circ T_1 \circ \cdots \circ T_{m-1}. \tag{9}$$

From Eq. (9), the difference equation for the unstable fixed point is described by

$$\boldsymbol{\xi}(k+m) = \boldsymbol{A}\boldsymbol{\xi}(k) + \boldsymbol{B}\boldsymbol{u}(k), \tag{10}$$

where

$$\begin{aligned}\boldsymbol{A} &= \boldsymbol{A}_{m-1}\boldsymbol{A}_{m-2}\cdots\boldsymbol{A}_2\boldsymbol{A}_1\boldsymbol{A}_m,\\ \boldsymbol{B} &= \boldsymbol{A}_{m-1}\boldsymbol{A}_{m-2}\cdots\boldsymbol{A}_2\boldsymbol{A}_1\boldsymbol{B}_m.\end{aligned} \tag{11}$$

The derivative of the Poincaré map $\boldsymbol{A}$ is equal to the product of the derivative of the maps T_k:

$$\boldsymbol{A} = \left.\frac{\partial T}{\partial \boldsymbol{x}_0^*}\right|_{t=\tau} = \prod_{k=0}^{m-1}\left.\frac{\partial T_k}{\partial \boldsymbol{x}_k^*}\right|_{t=\tau_k}, \tag{12}$$

$$\frac{\partial T_k}{\partial \boldsymbol{x}_k^*} = \left[\boldsymbol{I}_n - \frac{1}{\dfrac{\partial q_k}{\partial \boldsymbol{x}}\boldsymbol{f}_k}\boldsymbol{f}_k\frac{\partial q_k}{\partial \boldsymbol{x}}\right]\frac{\partial \boldsymbol{\varphi}_k}{\partial \boldsymbol{x}_k^*}, \tag{13}$$

where at least one of the characteristic multipliers of $\boldsymbol{A}$ is unstable by assumption, and $\boldsymbol{I}_n$ is the $n\times n$ identity matrix.

Now, we design the controller at the $(n-1)$-dimensional local section Π_0. Assume that Σ is an $(n-1)$-dimensional local coordinate in Π_0. Then $\boldsymbol{w}\in\Sigma\subset\boldsymbol{R}^{n-1}$ is given by

$$x_{01} = w_1, \cdots, x_{0(n-1)} = w_{n-1}, x_{0n} = s(w_1, \cdots, w_{n-1}). \tag{14}$$

We define the parameterization h^{-1} as

$$\begin{aligned}&h^{-1} : \Sigma \to \Pi_0\\ &\boldsymbol{w} \mapsto h^{-1}(\boldsymbol{w}) = (w_1, \cdots, w_{n-1}, s(w_1, \cdots, w_{n-1}))\end{aligned}. \tag{15}$$

where s is the function derived from Eq. (2). We also define the projection h as follows:

$$\begin{aligned}h \;:\; &\Pi_0 \to \Sigma\\ &(x_{01}, \cdots, x_{0n}) \mapsto (x_{01}, \cdots, x_{0(n-1)}).\end{aligned} \tag{16}$$

Then, the Poincaré map T_ℓ in Σ is expressed as

$$\begin{aligned}T_\ell \;:\; &\Sigma \to \Sigma\\ &\boldsymbol{w} \mapsto h\circ T\circ h^{-1}(\boldsymbol{w}).\end{aligned} \tag{17}$$

The difference equation in Σ is obtained as

$$\boldsymbol{\xi}'(k+1) = \boldsymbol{A}'\boldsymbol{\xi}'(k) + \boldsymbol{B}'\boldsymbol{u}(k), \tag{18}$$

where

$$\begin{aligned}\boldsymbol{A}' &= \frac{\partial T_\ell}{\partial \boldsymbol{w}_0} = \frac{\partial h}{\partial \boldsymbol{x}}\frac{\partial T}{\partial \boldsymbol{x}_0}\frac{\partial h^{-1}}{\partial \boldsymbol{w}},\\ \boldsymbol{B}' &= \frac{\partial T_\ell}{\partial \boldsymbol{\lambda}_0} = \frac{\partial h}{\partial \boldsymbol{x}}\frac{\partial T}{\partial \boldsymbol{\lambda}_0}.\end{aligned} \tag{19}$$

Stabilities of the fixed point and the periodic points are calculated by the characteristic multipliers of the characteristic equation

$$\left|\boldsymbol{A}' - \mu\boldsymbol{I}_{n-1}\right| = 0. \tag{20}$$

We construct the state feedback matrix $\boldsymbol{C}'$ such that $\boldsymbol{\xi}'(k)$ becomes stable:

$$\boldsymbol{u}(k) = \boldsymbol{C}'^{\top}\boldsymbol{\xi}'(k) = \boldsymbol{C}'^{\top}(\boldsymbol{w}(k) - \boldsymbol{w}^*), \tag{21}$$

where $\boldsymbol{C}'$ is the control gain $(r \times (n-1))$.

Based on $\boldsymbol{\xi}$, we may assign only $(n-1)$ poles. The controlled system and the characteristic equation can be expressed as

$$\frac{d\boldsymbol{x}}{dt} = \boldsymbol{f}_k(\boldsymbol{x}, \boldsymbol{\lambda}, \boldsymbol{\lambda}_0^* + \boldsymbol{C}'^{\top}\boldsymbol{\xi}, \boldsymbol{\lambda}_k), \quad k = 1, 2, \cdots, m-1, \tag{22}$$

$$\left| \boldsymbol{A}' + \boldsymbol{B}'\boldsymbol{C}'^{\top} - \mu \boldsymbol{I}_{n-1} \right| = \boldsymbol{0}. \tag{23}$$

From Eq. (23), the orbit is stabilized by the conventional linear control technique with stable pole assignment for any target unstable fixed point. To do so, as is well known, if the controllability condition of Eq. (19) is satisfied, i.e.,

$$\text{rank}\left[\boldsymbol{B}' \middle| \boldsymbol{A}'\boldsymbol{B}' \middle| \boldsymbol{A}'^2\boldsymbol{B}' \middle| \cdots \middle| \boldsymbol{A}'^{n-1}\boldsymbol{B}'\right] = n-1, \tag{24}$$

then Eq. (1) can be stabilized by the state feedback of Eq. (21).

The control input is added to the system only when the following condition is satisfied:

$$||\boldsymbol{x} - \boldsymbol{x}_0^*|| < \delta, \quad \delta > 0. \tag{25}$$

From the ergodic characteristics of the chaotic attractor, we expect that the orbit eventually visits this neighborhood within a reasonable time interval. When the orbit reaches the δ-neighborhood of the unstable fixed point, then it is stabilized by applying the control parameter perturbation described above.

3 Controlling Chaos of the Alpazur Oscillator Containing a State-depended Switch

3.1 System description

Consider the experimental control of the Alpazur oscillator containing a sate-dependent switch, as shown in Fig. 2 [Kawakami & Lozi, 1992].

Note that this circuit has a switch and a nonlinear resistor. This ensures that it is impossible to obtain fixed or periodic points by using the exact solution. After rescaling, we obtain

$$\tau = \frac{1}{\sqrt{LC_1}}t, \tag{26}$$

and the circuit equations become:

$$\text{SW:a} \begin{cases} \dfrac{di}{d\tau} &= -\sqrt{\dfrac{C_1}{L}}(ri + v) = F_0, \\ \dfrac{dv}{d\tau} &= \sqrt{\dfrac{L}{C_1}}(i - G(v) + \dfrac{E_1 - v}{R_0 + R_1}) = G_0, \end{cases} \tag{27}$$

and

$$\text{SW:b} \begin{cases} \dfrac{di}{d\tau} &= -\sqrt{\dfrac{C_1}{L}}(ri + v) = F_1, \\ \dfrac{dv}{d\tau} &= \sqrt{\dfrac{L}{C_1}}(i - G(v) + \dfrac{E_2 - v}{R_0 + R_2}) = G_1, \end{cases} \tag{28}$$

where the characteristics of the nonlinear resistor is assumed as

$$G(v) = -a_1 v + a_3 v^3. \tag{29}$$

Next, we define the function of the switch. The orbit is trapped within two half-planes, H and B, and changed at their boundaries:

$$\begin{aligned} H &= \{(i,v) \in \boldsymbol{R}^2 \,|\, v > h\}, \\ B &= \{(i,v) \in \boldsymbol{R}^2 \,|\, v < b\}, \\ \partial H &= \{(i,v) \in \boldsymbol{R}^2 \,|\, v = h\}, \\ \partial B &= \{(i,v) \in \boldsymbol{R}^2 \,|\, v = b\}. \end{aligned} \tag{30}$$

Assume that $b > h$. Then, the half-planes H and B have an overlapped region: $h < v < b$.

Two positions of the switch are interchanged each other on the boundaries. That is, if the flow on H reaches ∂H, then it changes into the flow on B. In the same way, if the flow on B reaches ∂B, then it changes into the flow defined on H. Assume that the solutions on H and B are defined as follows:

$$H \begin{cases} i(\tau) &= \varphi_0(\tau, i, v, E_1) \\ v(\tau) &= \phi_0(\tau, i, v, E_1), \end{cases} \tag{31}$$

$$B \begin{cases} i(\tau) &= \varphi_1(\tau, i, v, E_2) \\ v(\tau) &= \phi_1(\tau, i, v, E_2). \end{cases} \tag{32}$$

The behavior of the trajectory is sketched in Fig. 3.

Next, we choose the following parameters:

$$\begin{aligned} &L = 50[\mathrm{mH}], C_1 = 0.1[\mu F], E_1 = 2.04[\mathrm{V}], \\ &E_2 = 5.19[\mathrm{V}], r = 70.72[\Omega], V_{\mathrm{ref}} = -1.16[\mathrm{V}], \\ &R_0 = 0[\Omega], R_1 = 986[\Omega], R_2 = 280[\Omega], \\ &R_3 = 35.3[\mathrm{k}\Omega], R_4 = 150[\mathrm{k}\Omega], \\ &h = -2.61[\mathrm{V}], b = -0.26[\mathrm{V}], a_1 = 2.145 \times 10^{-3},\ a_3 = 6.9 \times 10^{-5}, \end{aligned} \tag{33}$$

the orbit of the circuit is a chaotic attractor, as shown in Fig. 5 (a), and also in Fig. 6 (a) of [Kousaka *et al.*, 1999].

In this paper, we choose $E_2 \in \boldsymbol{R}$ as the control parameter. We study the control of the UPO in by both numerical and experimental simulations, as will be shown below.

3.2 Design of a controller in the Alpazur oscillator

In this subsection, we explain the control method for stabilizing the unstable 1-periodic orbit.

We define the local sections Π_0 and Π_1 by using the scalar functions q_0 and q_1:

$$\begin{aligned} \Pi_0 &= \{\boldsymbol{w} \in B \mid q_0(i,v) = v - b = 0\} \\ \Pi_1 &= \{\boldsymbol{w} \in H \mid q_1(i,v) = v - h = 0\} \end{aligned} \tag{34}$$

The local mappings are naturally defined at the break points Π_0 and Π_1:

$$\begin{array}{rlcl} T_0: & \Pi_0 & \rightarrow & \Pi_1 \\ & i_0^* & \mapsto & i_1^* = \varphi_0(\tau_0, i_0^*, v_0^*, E_1^*) \\ & v_0^* & \mapsto & v_1^* = h \\ T_1: & \Pi_1 & \rightarrow & \Pi_0 \\ & i_1^* & \mapsto & i_2^* = \varphi_1(\tau_1, i_1^*, v_1^*, E_2^*) \\ & v_1^* & \mapsto & v_2^* = b. \end{array} \tag{35}$$

Then, we can define the Poincaré mapping as follows:

$$T = T_1 \circ T_0. \tag{36}$$

With the projection p and the parameterization p^{-1} defined by

$$\begin{array}{rlcll} p: & \Pi_0 & \rightarrow & \Sigma_0, & \boldsymbol{x}_0^* = \left[\begin{array}{c} i_0^* \\ v_0^* \end{array} \right] \mapsto w^* = i_0^*, \\ p^{-1}: & \Sigma_0 & \rightarrow & \Pi_0, & w^* = i_0^* \mapsto \boldsymbol{x}_0^* = \left[\begin{array}{c} i^* \\ b \end{array} \right], \end{array} \tag{37}$$

the Jacobian of the Poincaré mapping is obtained as follows:

$$\begin{aligned} A' = DT(\boldsymbol{w}_0) &= \frac{\partial p}{\partial \boldsymbol{x}} \frac{\partial T}{\partial \boldsymbol{x}_0^*} \frac{\partial p^{-1}}{\partial \boldsymbol{w}} \\ &= \left(\begin{array}{c} \dfrac{\partial \varphi_0}{\partial i_0^*} - \dfrac{F_0}{G_0} \dfrac{\partial \phi_0}{\partial i_0^*} \end{array} \right) \left(\begin{array}{c} \dfrac{\partial \varphi_1}{\partial i_1^*} - \dfrac{F_1}{G_1} \dfrac{\partial \phi_1}{\partial i_1^*} \end{array} \right). \end{aligned} \tag{38}$$

Finally, we construct the following state feedback $u(k) \in \boldsymbol{R}$:

$$u(k) = C'(i(k) - i^*), \tag{39}$$

where C' is the control gain. Using this controller, the orbit can be stabilized due to the linear control technique with stable pole assignment.

The location of the UPPs, their multipliers, and the control gains are shown in Table1.

In this example, we place the poles to realize dead-beat control. The response of the control signal and the behavior of the controlled Alpazur oscillator is sketched in Fig. 4.

Note that the characteristic multiplier on the local section Π_0 of the target orbit is bigger than unity (see Table 1). Thus, in the simulation figure, when the chaotic attractor (the controlled orbit) exists around the UPO (the target orbit), the term $u(k)$ is always added to the control parameter as a perturbation. However, if the position of the switch is b, the controller is turned off, because we choose E_2 as the control parameter in this situation.

3.3 Numerical and experimental results

Using the information of Section 3.2, we consider the control of chaos by means of both numerical simulation and experimental circuitry.

The control unit is easily realized by the window comparator, sample-hold circuits, and so on. Figure 7 shows a circuit realization of the control unit. We connect the inductor with the resistor r

and we control the voltage value. First, since the current value is small, we amplify it by using the microscopic signal amplifier. Next, the input voltage is sampled by the sample-hold circuit at every cycle. The output voltage u_k of the sample-hold circuit is subtracted with the unstable fixed point i^*. Finally, the output voltage u_k sums the DC voltage E_2 with the summing amplifier. As a result, we can generate the state feedback $u_k + E_2$.

Now, the system has a chaotic attractor until the orbit visits the vicinity of the unstable fixed point (see Fig. 5 (a) and Fig. 6 (a)). After that, the state feedback given by Eq. (39) is added to the control parameter E_2 when the orbit visits the neighborhood of the unstable fixed point, namely, when the following condition is satisfied:

$$||i - i^*|| < \delta. \tag{40}$$

where δ should be sufficiently large unless the linearization is invalid.

We chose $\delta = 0.1$[mA] in this example. Figures 5 (b) and (c) show the computer simulations of the stabilized 1- and 2-periodic orbits, respectively. In the same way, the unstable 1- and 2-periodic orbits in the chaotic attractor are stabilized in laboratory experiments (see Figs. 6 (b) and (c)).

The above target orbit is a chaotic attractor generated via cascading the period-doubling bifurcations. When the parameter E_1 decreases from this area, the chaotic attractor changes to another chaotic attractor via global bifurcation [Kousaka *et al.*, 1999]. Figure 8 (a) shows this chaotic attractor.

Finally, we control the unstable 1-periodic orbit in the attractor, but we fix the location of the unstable 1-periodic orbit and the control gain as shown in Table 1. In this case, the chaotic attractor is also stabilized to a 1-periodic orbit, as shown in Fig. 8 (b). Figure 8 (c) shows the transition from the chaotic attractor to the 1-periodic orbit.

From the experimental results, we found that the control is robust within about 10 percent perturbation to the input voltage E_2.

4 Concluding Remarks

We have proposed and investigated an effective control method for stabilizing the chaotic attractor to UPOs in a nonlinear dynamical system containing a state-dependent switch. We have derived a composite mapping as the Poincaré mapping and designed the controller in the $(n-1)$-dimensional local section. As an example, we have considered the task of controlling chaos in the Rayleigh-type oscillator with a state-dependent switch. The unstable 1- and 2-periodic orbits were stabilized by the designed controller, and were verified by both numerical simulation and laboratory experiment.

In this paper, we only dealt with the two-dimensional piecewise nonlinear systems. However, this control method can be applied to general interrupted electric circuits. We are currently applying the method to higher-dimensional systems (circuits) and investigating its stabilization capability and performance.

References

[Bernardo & Chen, 1999] Bernardo, M. di & Chen, G. [1999] "Controlling bifurcations in nonsmooth dynamical systems," in *Controlling Chaos and Bifurcations in Engineering Systems*, Chen, G. (Ed.), CRC Press, Boca Raton, FL, USA, 391-416.

[Bernardo, 2000] Bernardo, M. di. [2000] "Controlling switching systems: A bifurcation approach," in *Proc. IEEE ISCAS*, 377–380.

[Bueno & Marrero, 2000] Bueno, R. S. & Marrero, J. L. R. [2000] "Application of the OGY method to the control of chaotic DC-DC converters: Theory and experiments," in *Proc. IEEE ISCAS*, 369–372.

[Chen & Dong, 1993] Chen, G. & Dong, X. [1993] "From chaos to order — Perspectives and methodologies in controlling chaotic nonlinear dynamical systems," *Int. J. of Bifurcation and Chaos*, **3**(6), 1363–1409.

[Hunt, 1991] Hunt, E. R. [1991] "Stabilizing high-period orbits in a chaotic system: The diode resonator," *Phys. Rev. Lett.*, **67**, 1953–1955.

[Kawakami & Lozi, 1992] Kawakami, H. & Lozi, R. [1992] "Switched dynamical systems — Dynamical of a class of circuits with switch —," *Proc. RIMS Conf.* "Structure and Bifurcations of Dynamical Systems," Ushiki, S. (Ed.), World Scientific, Singapore, 39–58.

[Kousaka *et al.*, 1999] Kousaka, T., Ueta, T. & Kawakami, H. [1999] "Bifurcation of switched nonlinear dynamical systems," *IEEE Trans. Circuits and Systems-II*, **46**(7), 878–885.

[Kousaka *et al.*, 2001] Kousaka, T., Ueta, T. & Kawakami, H. [2001] "Chaos in a simple hybrid system and its control," *Electron. Lett.*, **37**(1), 1–2.

[Ott *et al.*, 1990] Ott, E., Grebogi, C. & Yorke, J. A. [1990] "Controlling chaos," *Phys. Rev. Lett.*, **64**, 1196–1199.

[Poddar *et al.*, 1995] Poddar, G., Chakrabarty, K. & Banerjee, S. [1995] "Experimental control of chaotic behavior of buck converter," *IEEE Trans. Circuits and Systems*, **42**(8), 502–504.

[Pyragas, 1992] Pyragas, K. [1992] "Continuous control of chaos by self-controlling feedback," *Phys. Lett. A*, **170**, 421–428.

[Saito & Mitsubori, 1995] Saito, T. & Mitsubori, K. [1995] "Control of chaos from a piecewise linear hysteresis circuit," *IEEE Trans. Circuits and Systems*, **42**(12), 168–172.

[Ueta & Kawakami, 1995] Ueta, T. & Kawakami, H. [1995] "Composite dynamical system for controlling chaos," *IEICE Trans. Fundamentals*, **E77-A**(6), 708–714.

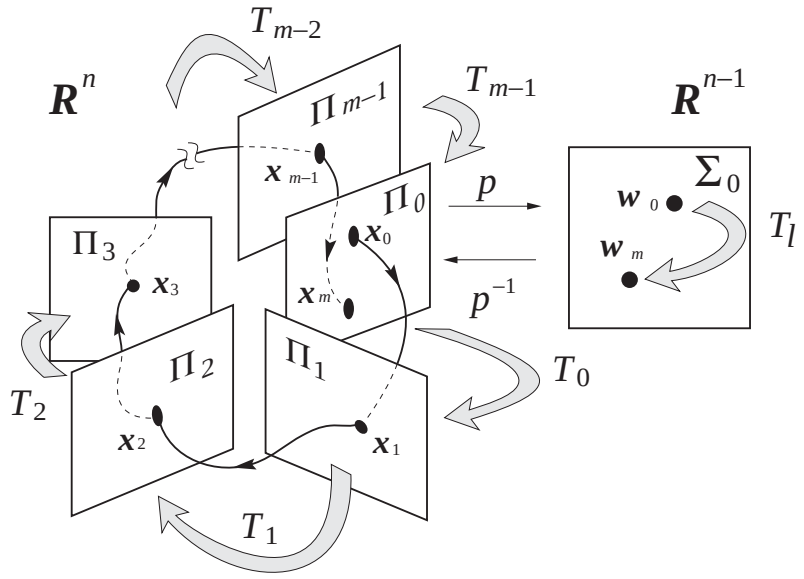

Figure 1: Example of the behavior of the trajectory in Eq. (1).

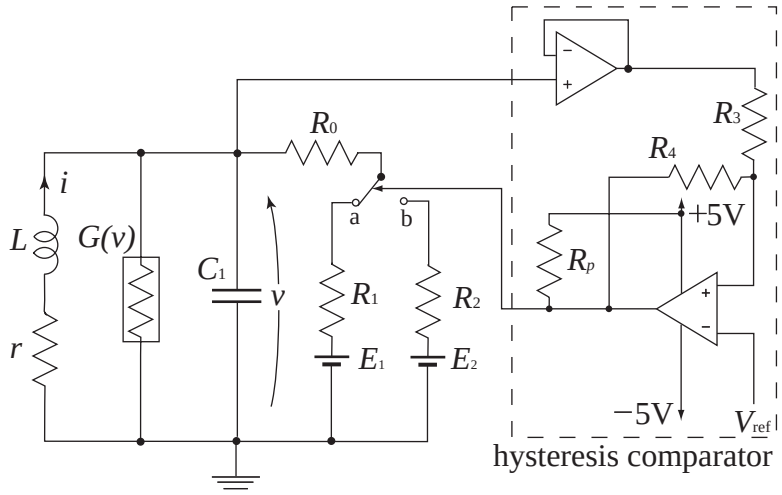

Figure 2: The Alpazur oscillator containing a state-dependent switch.

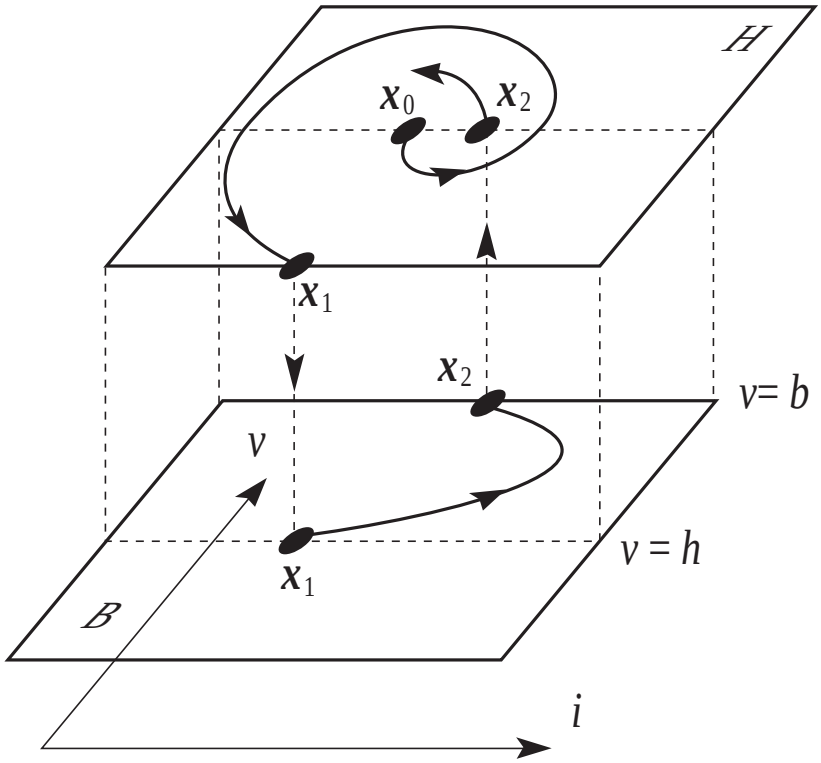

Figure 3: Example of the trajectory of the Alpazur oscillator.

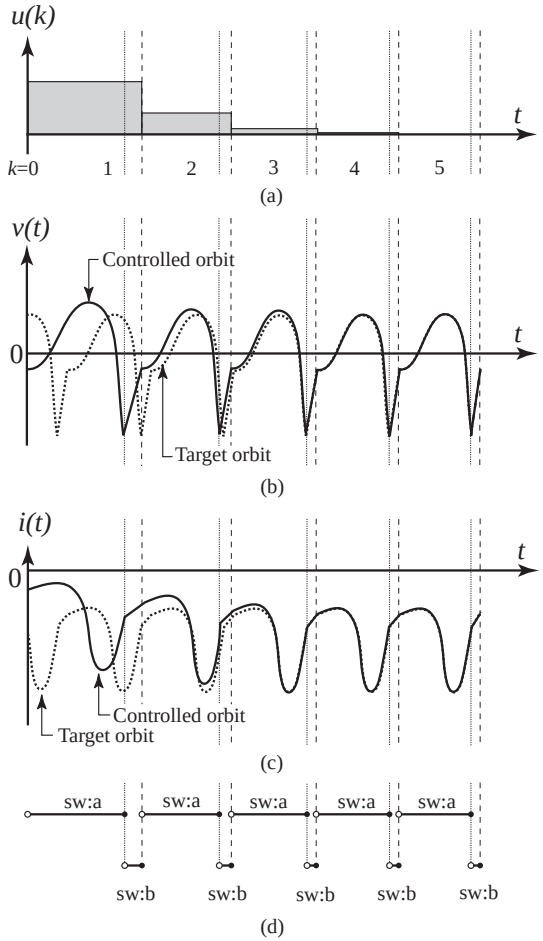

Figure 4: Response of the control signal and the controlled orbit. (a) State feedback $u(k)$. (b) Transient response of electric voltage $v(t)$. (c) Transient response of electric current $i(t)$. (d) Motion of the switch.

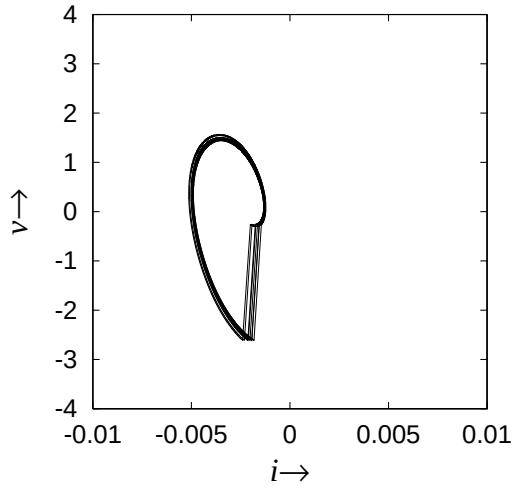

(a)

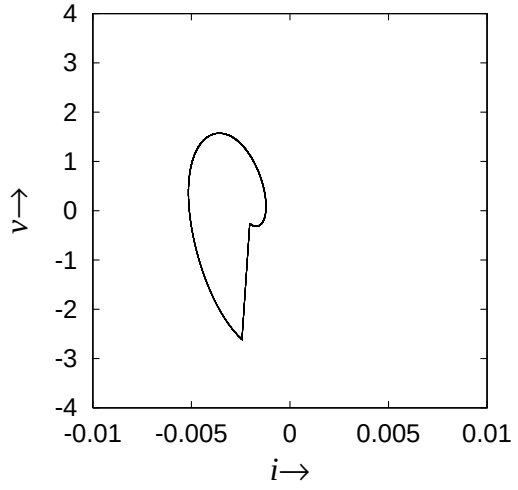

(b)

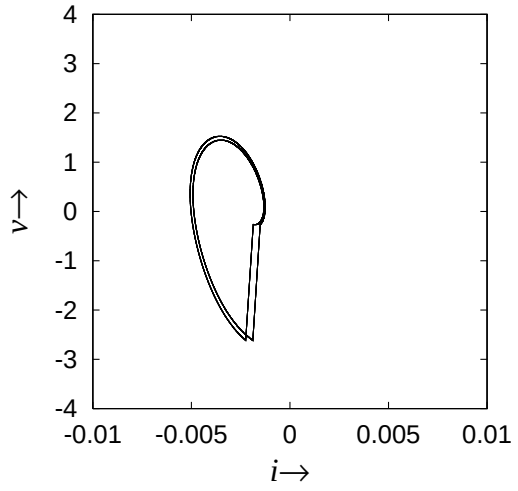

(c)

Figure 5: Computer simulations. (a) Chaotic attractor. (b) Stabilized 1-periodic orbit. (c) Stabilized 2-periodic orbit.

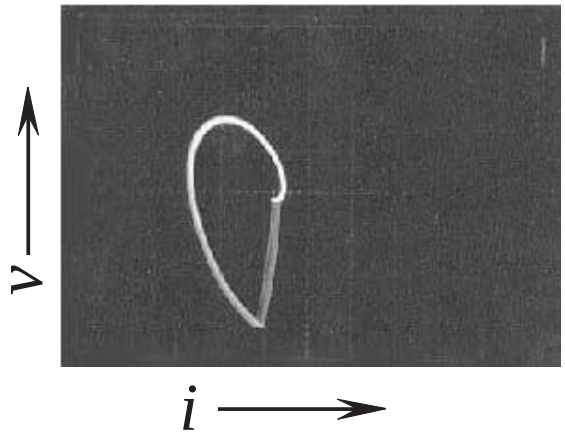

(a)

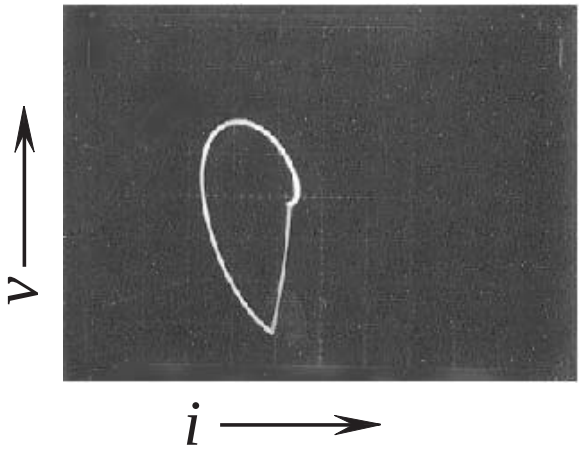

(b)

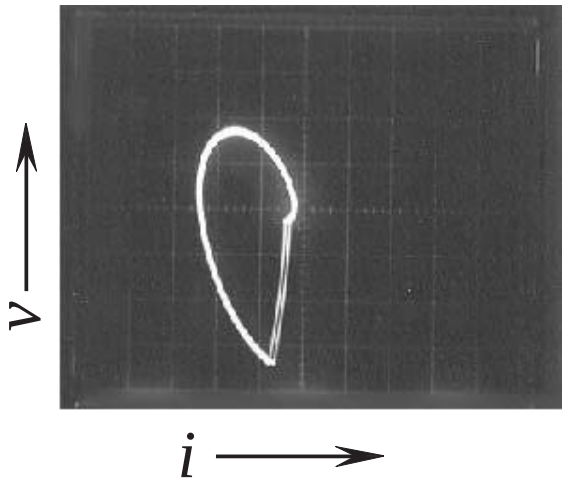

(c)

Figure 6: Laboratory experiments-1. (a) Chaotic attractor. (b) Stabilized 1-periodic orbit. (c) Stabilized 2-periodic orbit.

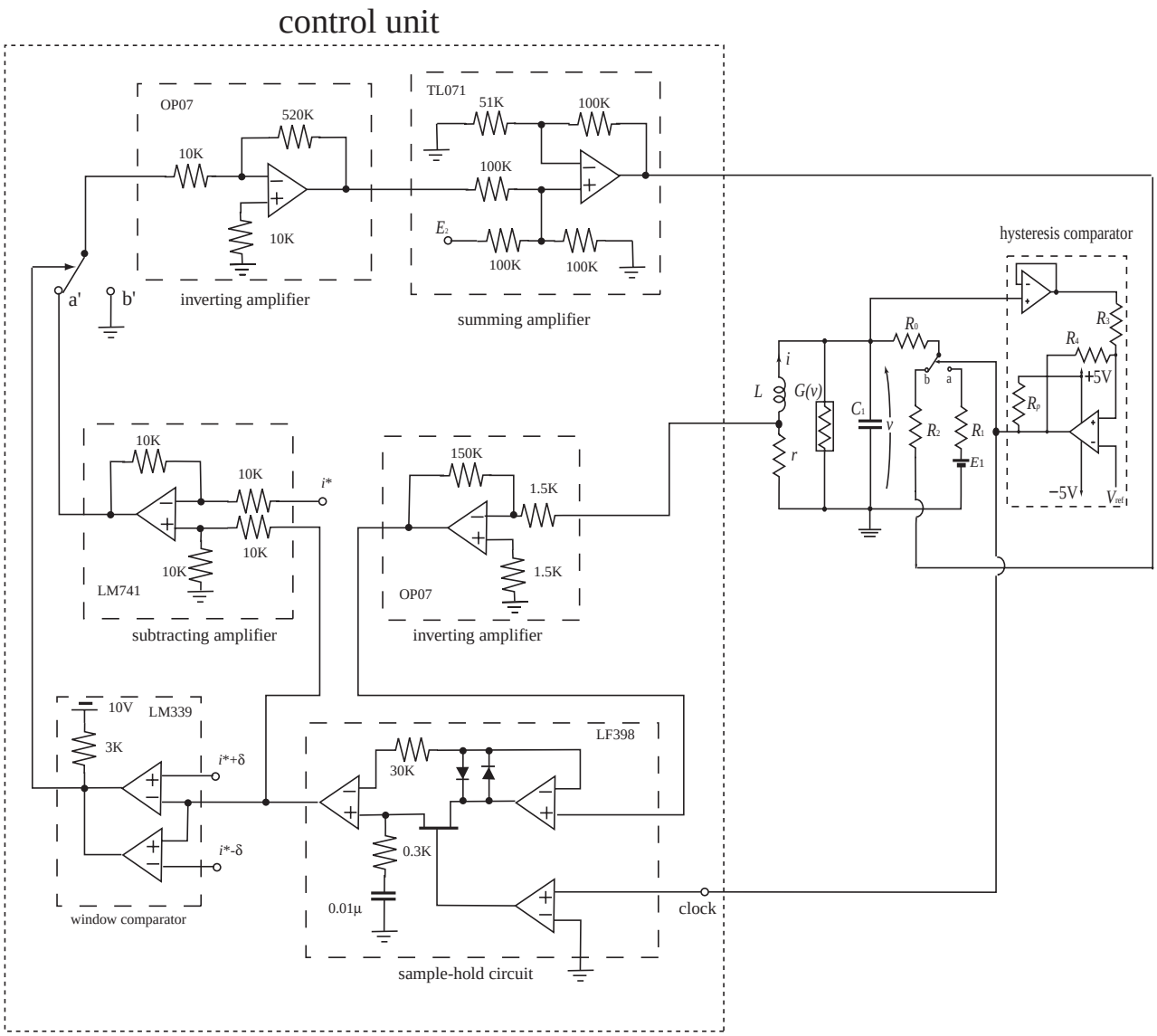

Figure 7: Circuit realization of the control unit.

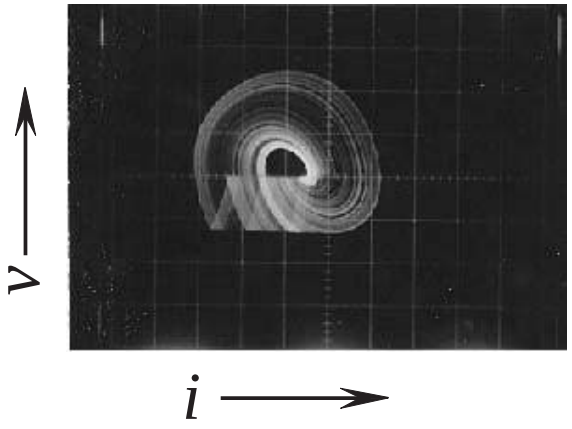

(a)

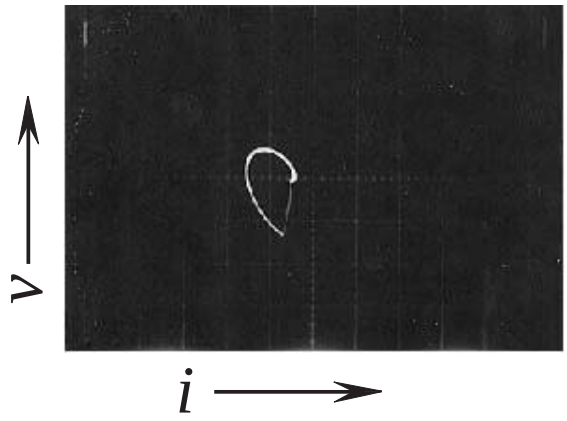

(b)

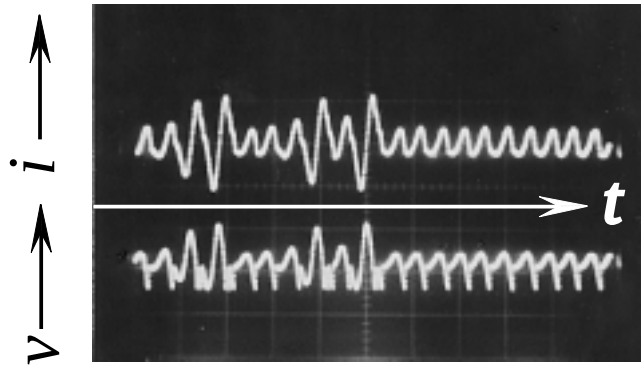

(c)

Figure 8: Laboratory experiments-2. (a) Chaotic attractor. (b) Stabilized 1-periodic orbit. (c) The transition from the chaotic attractor to stabilized 1-periodic orbit.

Table 1: Properties of the UPPs, characteristic multiplier, and control gain C'

Period	Location of the UPPs in Σ_0.($v^* = -0.26$[V])	Characteristic multiplier	Control gain C'
1	-2.041[mA]	-1.65	55699.5
2	-1.51[mA]	-2.08	-21419.6